PERSPECTIVE | FOCUS
https://doi.org/10.1038/s41567-020-0925-6

nature physics



# Topological superconductivity in hybrid devices

S. M. Frolov[1]✉, M. J. Manfra[2,3] and J. D. Sau[4]

**Topological superconductivity can emerge from the combination of conventional superconductivity in a metal and strong spin–orbit coupling in a semiconductor when they are made into a hybrid device. The most exciting manifestation of topological superconductivity is the Majorana zero modes that are predicted to exist at the ends of the proximatized nanowires. In this Perspective, we review the evidence for the existence of Majorana zero modes that has accumulated in numerous experiments and the remaining uncertainties, and discuss what additional evidence is desirable. One very important factor for future development is the quality of the interface between the superconductor and semiconductor; we sketch out where further progress in the materials science of these interfaces can take us. We then discuss the path towards applying these modes in topologically protected quantum computing and observing more exotic kinds of superconductivity based on the same materials platform, and how to make connections to high-energy physics.**

Topological superconductivity is distinct from other kinds of superconductivity in subtle yet profound ways. What makes it a crown jewel among non-interacting topological phases is its capacity to harbour states that are non-Abelian, so neither fermionic nor bosonic[1,2]. There is clearly a fundamental interest in understanding new classes of particles, but this field is made all the more important by the potential applications that these non-Abelian states have in fault-tolerant quantum computing[3]. Topological superconductivity can emerge intrinsically in the bulk of a material[4], or it can be induced at an interface between two materials[5]. Among the wide variety of platforms that have been proposed to host this effect, we focus on interfaces of two of the most common materials—a superconducting metal and a semiconductor. Even though neither of the constituents is topological by itself, the prediction is that topological superconductivity will emerge when ingredients such as particle–hole symmetry and spin–orbit interaction are borrowed from either side of the interface[6,7]. Using heterostructures of this form benefits from a long history of crystal growth and device fabrication of both superconductors and semiconductors, though aspects of their integration have introduced new challenges. A comprehensive suite of proposals lay out a pathway to generating, detecting and manipulating Majorana zero modes (MZMs), the most basic of non-Abelian anyons in these materials[8,9].

The usual way of introducing topological superconductivity is through Majorana zero modes which are edge, end or defect states. Here, we take a different route, and focus on a unique property of the topological phase as a whole: the fermion parity anomaly that is a hallmark of time-reversal symmetry-breaking topological superconductors[1,8]. We shall then motivate how this anomaly directly mandates MZMs at system boundaries. In the case of a proximatized semiconducting nanowire, the system boundaries refer to the two ends of the wire.

Let's start by considering a system without boundaries: a ring of a strictly one-dimensional and spinless superconductor. Fermions, of course, possess half-integer spin, but theoretically we are free to assume spinless particles whose creation operators still anticommute[8]. The wave functions are periodic around the ring, and momenta take discrete values including one at $k$=0 when flux through the ring is zero (Fig. 1a). In order to form Cooper pairs, the electrons favour pairing up with a partner that has opposite momentum. However, because these fermions have no spin, the state at $k$=0 has no partner to form a Cooper pair with. Therefore, this realizes a superconducting state with a single unpaired electron. This is already unusual for conventional (non-topological) superconductors because they are fully paired in the ground state. The fermion parity anomaly is exposed when we apply a quantum of magnetic flux through the ring. The boundary conditions change and the fermionic $k$=0 state disappears: all electrons now have a Cooper-pair partner (Fig. 1a). The fermion parity of the ground state has changed from odd to even: this is an anomaly. It has not been directly observed but may in principle be accessed through Coulomb blockade oscillations of conductance[10].

The genesis of Majorana modes takes place when the spinless superconducting ring is cut open, and thereby transformed into a one-dimensional wire. Imagine doing this by gradually inserting a barrier into the ring (Fig. 1b). As long as the barrier allows tunnelling, the fermion parity anomaly must persist, and the ground state parity should change upon insertion of flux. But the flux through the loop now controls the phase of the tunnelling amplitude: changing flux by a single quantum flips the tunnelling amplitude from $+t$ to $-t$. The transition from an even- to odd-parity ground state then requires there to be states with energies of order $t$[8]. In the limit of infinitely small $t$ these are zero energy states bound to the ends as a consequence of topological fermion parity anomaly: they are the MZMs.

While spinless fermions do not exist, one strategy to obtain an effectively spinless superconductor is to spin-polarize all the electrons. But conventional singlet superconductivity requires pairing of electrons of opposite spin to preserve time-reversal symmetry, thus making the most common superconductors unsuitable for hosting MZMs. A workaround is to induce superconductivity in a spin-polarized semiconductor using the proximity effect with a spin-singlet superconductor (Fig. 1c)[6,7]. If there is a mechanism for the spins of the electrons to rotate as they cross the interface, conventional Cooper pairs may tunnel into the semiconductor. The external magnetic field required to polarize semiconductors such as InAs or InSb, with their large effective Lande $g$-factors, is low enough to preserve superconductivity in thin films of Al or Nb. And spin–orbit interaction within InAs or InSb is large enough to break the perfect spin-polarization which allows the tunnelling Cooper pairs to rotate from singlet to triplet.

In order to localize MZMs it is necessary to implement a one-dimensional system, such as a nanowire (Fig. 1c). Initially, semiconductor nanowires grown via vapor–liquid–solid phase

[1]Department of Physics and Astronomy, University of Pittsburgh, Pittsburgh, PA, USA. [2]Department of Physics and Astronomy, Purdue University, West Lafayette, Indiana, USA. [3]Microsoft Quantum Purdue, Purdue University, West Lafayette, Indiana, USA. [4]Department of Physics, University of Maryland, College Park, MD, USA. ✉e-mail: frolovsm@pitt.edu

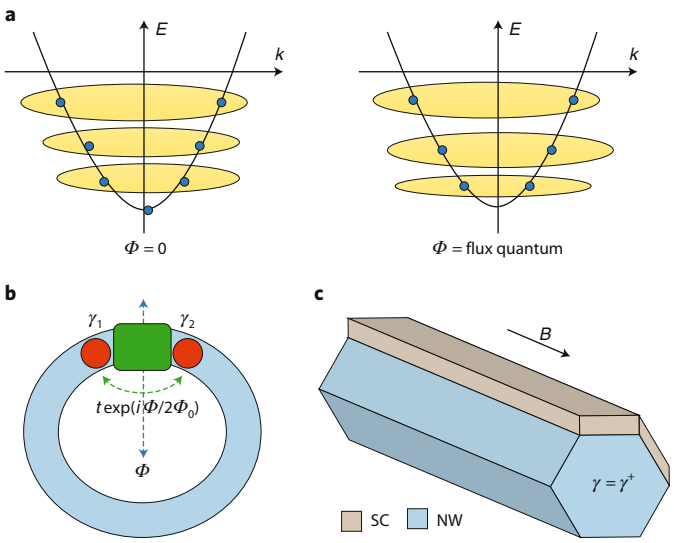


**Fig. 1 | The concept of topological superconductivity using a spinless superconductor primer. a**, Fermion parity anomaly in a ring of a spinless superconductor. When no external flux threads the ring, the ground state of a spinless superconductor features a single unpaired fermion at $k$=0. When a single flux quantum is applied, the ground state is fully paired with even total parity. $E$, energy; $k$, wavevector. **b**, MZMs (red circles) are nucleated in a spinless superconductor ring when a tunnel barrier (green) is introduced, with a flux-dependent tunnelling amplitude $t(\phi)$. **c**, the ingredients of an effective spinless superconductor considered here are the strong spin–orbit semiconductor nanowire (NW) coupled to a conventional superconductor (SC) in an external magnetic field $B$. MZMs $\gamma$ are expected at the ends of the nanowire.

epitaxy coupled to *s*-wave superconductors ex situ (in a separate fabrication process) were used. But new approaches to growth such as integrating epitaxial superconducting layers in situ[11–13], and developing planar superconductor/two-dimensional electron gas hybrids as well as selective area growth of superconductor–semiconductor wire networks[14,15] may advance progress towards unambiguous demonstration of MZMs, and facilitate experiments requiring more complex geometries.

Superconducting proximity effects in low-dimensional semiconductors had been studied for two decades prior to the first wave of Majorana experiments in 2012, but most experiments used close-to-zero applied magnetic field, and thus not in the spin-polarized regime. Following the predictions of Majorana modes in 2010[6,7], experiments at finite field were quickly performed on semiconductor nanowire devices. They largely focused on identifying zero voltage bias conductance peaks at the ends of the nanowire, as these indicate the presence of localized states that the community hoped were the MZMs[16–20]. It was quickly realized that the observed peaks did not clearly correspond to any previously known phenomenon (Fig. 2a). Their most striking feature was a zero-bias conductance peak pinning to zero bias voltage upon significant changes in magnetic field. Even though they appeared only at finite magnetic field, the resonances apparently lacked Zeeman energy—they behaved as spinless, zero-energy states—just as Majorana modes should.

The field took a surprise swing when it became clear that resonances that also do not shift from zero energy in a magnetic field were identified as being due to Andreev bound states (ABSs) in quantum dot devices (Fig. 2b)[21]. The similarities between ABSs and MZMs run deep: both phenomena correspond to low-energy (subgap) bound states near superconductor boundaries. In some senses, it is intriguing that a different physical effect could produce such similar phenomenology. As we have discussed, a long topologically superconducting wire is expected to have two strictly zero energy MZMs at the ends. But in a short wire, the wave functions of the two MZMs partially overlap so that their interaction gives them both a non-zero energy and therefore they become ABSs. In turn, regardless of whether the wire is topological or not, any ABS can be represented in the 'Majorana basis' or, in other words, split into two Majorana wave functions ('left' and 'right'; Fig. 2c). The two wave functions may fully overlap, which is the case for trivial ABS[22], or they may strongly overlap and are then known as partially separated Andreev or quasi-Majorana states[23]. The smooth nature of the barrier potential plays a crucial role in keeping such quasi-Majorana states near zero energy[24]. What is interesting is that quasi-Majorana states do not need to accompany a bulk topological phase, but may arise generically under similar conditions of strong spin–orbit coupling and large magnetic field[23,25]. An alternative source for non-topological zero-bias peaks is referred to as a 'class-D' peak[26,27]. Such a peak arises due to the level repulsion from other nearby states pushing some resonances to low bias. While class-D peaks generically exhibit less zero-bias pinning than MZMs, it is possible to find instances of considerable pinning through data selection[25].

In light of these realizations, improved nanowire devices were used to investigate more nuanced predictions for the properties of Majorana zero-bias peaks. Naturally, the main aim was to eliminate or separate out trivial ABSs so that the MZMs could be unambiguously identified. For example, signatures such as the $2e^2/h$ 'quantized' conductance, the topological phase diagram in Zeeman energy and chemical potential, near-zero bias oscillations of conductance resonances, the degree of zero-bias pinning for different length segments, and closing of the apparent superconducting gap were considered[28–33]. While each observation was consistent with MZMs, many were also reproduced without assuming MZMs[25,34]. A similar fate was in store for the efforts to demonstrate the fractional Josephson effect which at first was widely believed to be unique to MZMs[6,8,35]. The community has realized that this effect may not appear in a topological system due to dynamics effects such as quasiparticle relaxation and Landau–Zener transitions[6,36], and the latter also responsible for apparent fractional Josephson effect even in non-topological systems[37].

While, collectively, zero-bias conductance peaks were explored extensively, each individual experiment demonstrates only one or two of the predicted signatures of a MZM; no experiment found all expected features at the same time. Given that the similarities between ABSs and MZMs are so striking, the prospects of coming up with a clear single-figure 'smoking gun' evidence of a MZM is unlikely. Instead, a comprehensive set of internally consistent measurements performed on the same sample is needed to unambiguously establish the existence of Majorana modes. One advantage of the super-semi system is in the large number of control parameters that allow for elaborate testing of the MZM hypothesis: through gate voltages, magnetic field magnitude and orientation, device geometry, materials and interface tailoring.

One property which may, if clearly demonstrated, definitively distinguish an ABS from a MZM is the non-local nature of Majorana wave functions, which is the correlation between left and right MZM. Experiments that have been conducted so far are primarily two-terminal measurements, and the all imply some degree of non-locality. Recently, experiments began to appear in three-terminal devices (Fig. 2d)[33,38,39], where near-zero energy states on the two ends of a nanowire can be probed independently. Alternatively, such three-terminal devices can be used to probe signatures of the topological quantum phase transition such as quantized heat conductance[40] and non-local rectifying electrical conductance[41]. Proposals for Majorana teleportation and noise correlation measurements, and also Majorana mode interferometry, are some of the future experiments that require MZM nonlocality[42,43].

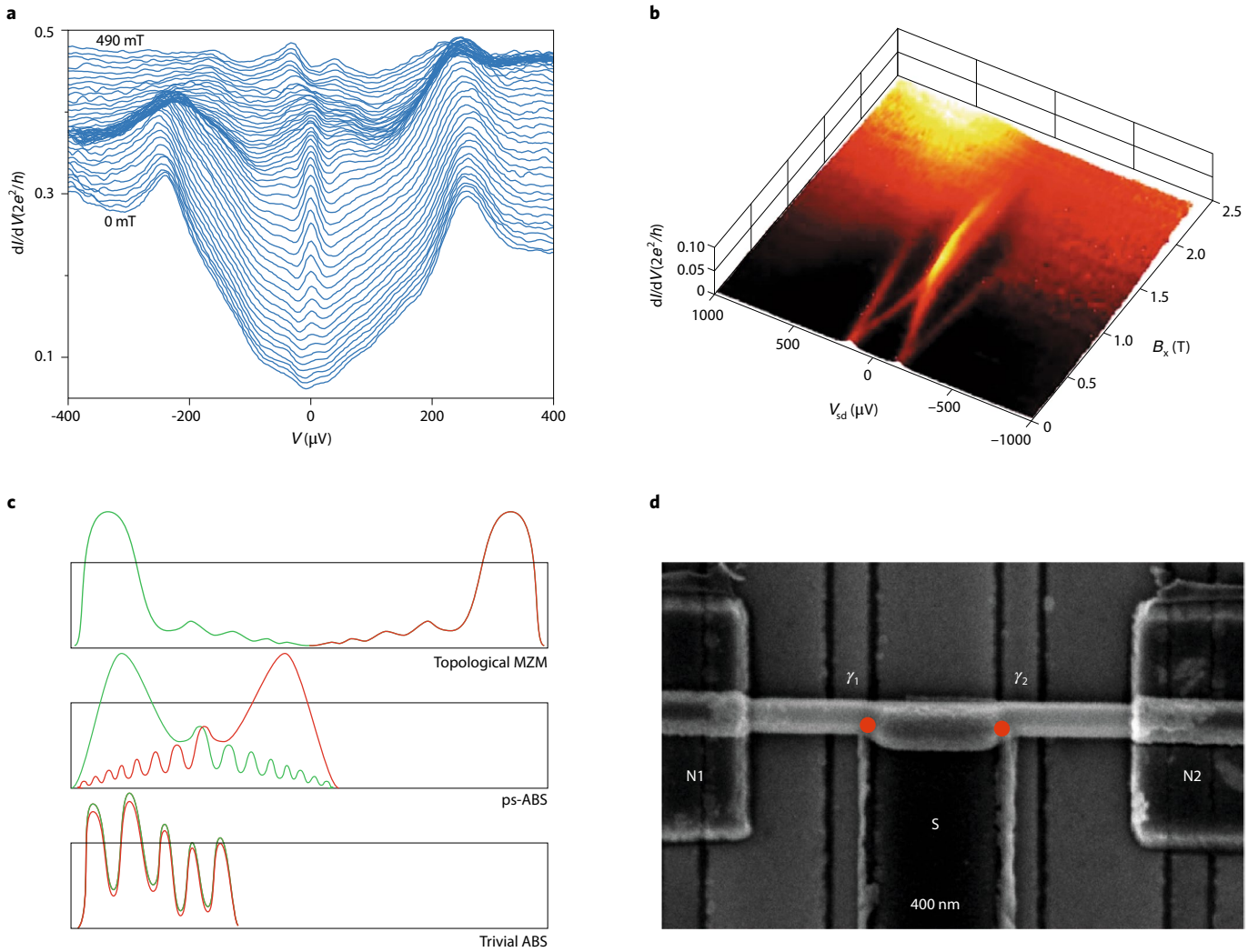


**Fig. 2 | Zero-bias conductance peaks can appear due to MZMs or due to trivial ABSs. a**, Zero-bias conductance peaks emerging at finite magnetic field as reported by one of the 2012 nanowire experiments[16]. **b**, Another zero-bias peak appearing at a confluence of two resonances at a finite field. These data appear in the supplementary materials of ref. [21] where a quantum dot device not capable of sustaining MZMs was studied. **c**, Subgap wave functions in a semiconductor nanowire coupled to a superconductor decomposed in left Majorana (green) and right Majorana (red) basis. Three situations are presented: well-separated topological MZMs (top), partially separated Andreev bound states (ps-ABS; middle), completely trivial ABSs (bottom) where green and red wave functions fully overlap. **d**, A three-terminal nanowire device designed to probe the left and right end of a superconductor–semiconductor segment S via normal probes N1 and N2[39]. *I*, current; *V*, voltage; *e*, electronic charge; *h*, Planck constant; $V_{sd}$, source–drain voltage; $B_x$, magnetic field along the nanowire. Approximate positions of MZMs $\gamma_1$ and $\gamma_2$ are indicated by red circles. Figure adapted with permission from: **a**, ref. [16], AAAS; **b**, ref. [21], Springer Nature Ltd; **d**, ref. [39].

Topological superconductivity at superconductor–semiconductor interfaces is strongly dependent on the materials that the device is constructed from and the properties of the interface. In contrast with conventional superconductivity, topological superconductivity is highly sensitive to any disorder, including scattering on non-magnetic impurities[44]. Intrinsic material parameters such as band offsets at the interfaces, which are not well known at present, may influence whether the system is close to or far from the theoretical single one-dimensional channel limit. The effective *g*-factor and spin–orbit coupling at the interface may also be modified, which would have an impact on the formation and stability of a topological phase. Lattice mismatch and changes of crystal symmetry between the superconductor and semiconductor are also important. While these concerns are specific to superconductor–semiconductor systems, we expect detailed materials considerations to be key for all attempts to implement topological superconductivity.

One of the recent highlights with large potential for the future is the development of two dimensional superconductor–semiconductor heterostructures. Clean interfaces are created between an *s*-wave superconductor (typically aluminum) and a two-dimensional electron gas with strong spin–orbit coupling within the ultra-pure molecular beam epitaxy environment (Fig. 3a–c)[12,32]. The superconductor and the semiconductor can be separated by a thin tunnelling barrier to control the induced superconductivity. The most well developed materials for the semiconductor to date are InAs or InSb, but both of these require heteroepitaxy on lattice-mismatched surfaces. Therefore, inclusion of extended defects is inevitable and must be effectively managed to ensure that the quality of the devices is high. The first devices made out of these heterostructures featured one-dimensional channels defined either via top-down etching, or within a Josephson junction[31,45,46]. Experiments on those devices showed zero bias conductance peaks qualitatively similar to those

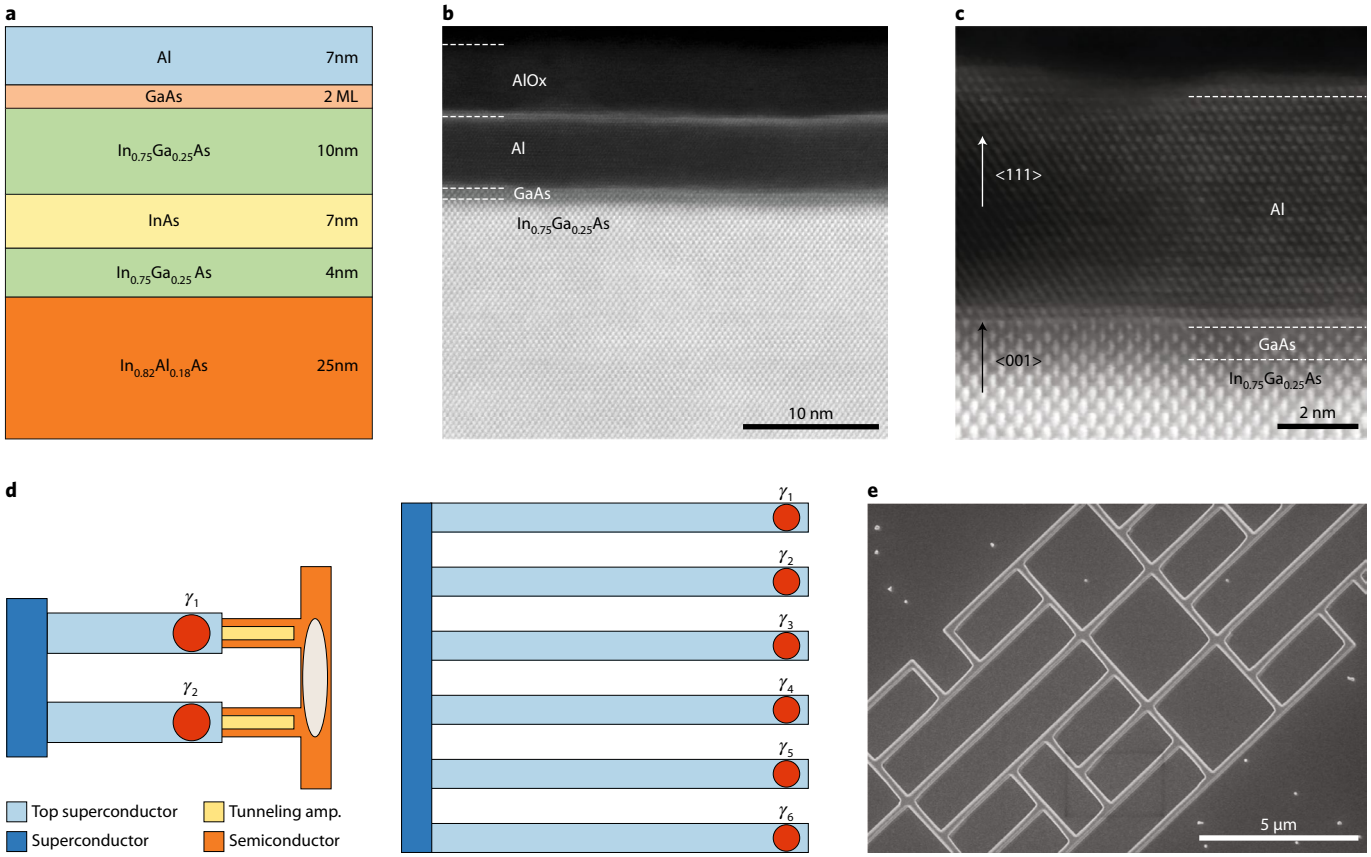


**Fig. 3 | Materials considerations for superconductor/semiconductor hybrid systems. a**, Schematic stack of planar Al/InAs structure similar to that used in ref. [31]. ML, monolayer. **b**, Scanning transmission electron microscopy image of the InAs quantum well region, including 10 nm InGaAs barrier and 7 nm epitaxial aluminum. **c**, High-resolution scanning transmission electron microscope image demonstrating epitaxial arrangement at the superconductor/semiconductor interface. The (111) planes of aluminum are parallel to the (001) planes of the III–V semiconductor, transitioning at an abrupt interface. **d**, Schematic building blocks of topological nanowire networks required for proposed topological quantum computing schemes as in ref. [49]. **e**, Scanning electron microscopy image of an InAs nanowire array grown by selective area growth demonstrating the capacity to create complex networks. Panel **d** adapted with permission from ref. [49], APS. Images in **b**,**c** courtesy of R.E. Diaz.

observed in bottom-up grown nanowire-based devices, leaving the issue of separating MZMs and ABSs open for the moment.

To make sustained progress, the community will have to deepen understanding of the electronic properties specific to superconductor–semiconductor interfaces using a combination of theory and spectroscopy tools beyond electron transport. We expect that the established strengths of molecular beam epitaxy growth of semiconductor heterostructures, including in situ diagnostics, high chemical purity and interface control with monolayer precision may be leveraged to yield even lower defect density and interfaces maximally optimized for MZM generation.

Undeniably, the prediction of non-Abelian statistics of Majorana zero modes, and its potential utility for quantum information processing[3] is what continues to fuel the interest in topological superconductivity. The most intuitive way of understanding this property is by physically moving two MZMs around each other and observing that the ground state parity changes. Quantum information stored in the charge parity is protected against small perturbations for a subset of quantum logic operations, although not the full set that is required for universal quantum computation. Moving MZMs is technically challenging for Majorana modes bound to ends of wires. Fortunately, a combination of auxiliary Majorana wires together with measurements of the fermion parity—the so-called measurement-only approaches[47–50]—can emulate this. The variety and increasing level of detail in these proposals clearly sets the superconductor–semiconductor platform apart in the efforts to realize scalable topological quantum computing. However, these geometries are quite complex and difficult to realize with bottom-up grown nanowires or etching down two-dimensional heterostructures (Fig. 3d). Here, a selective-area growth strategy, if proven to produce material of sufficient quality, may find utility as it front loads the fabrication effort prior to epitaxial growth (Fig. 3e)[14,15,51–54]. The predetermined network is grown through a patterned dielectric mask deposited on a semiconductor substrate, so that superconductors can then be deposited in situ on predetermined wire facets. Exploration of selective area growth capabilities and the limitations of this approach is an active area of research.

Coherence of a Majorana qubit depends on the magnitude of the induced superconducting gap which is a measure of topological protection. It is also important to avoid non-equilibrium effects known as quasiparticle poisoning, which lead to fluctuations in charge parity and thereby scramble the two states of a Majorana qubit[55]. To date, aluminum is the preferred superconductor because of its relative resistance to quasiparticle poisoning. Indeed, in Coulomb-blockaded devices aluminum is the only known superconductor to produce 2*e*-periodic transport that also does not alter charge parity[28,56]. The superconducting gap of aluminum at zero magnetic field is 200 µeV (equivalent to 2 K) which gives the upper bound on any induced topological gap. Material parameters inherent to real superconductor/semiconductor interfaces will tend to

reduce the gap in the topological regime, perhaps significantly. Thus there is strong motivation to explore other superconductors that may enhance the topological gap while maintaining aluminum's desirable characteristic of 2*e*-periodic transport[57–59].

To summarize the short-term goals of the field, the immediate attention is likely to be focused on deeper understanding of the materials science of superconductor-semiconductor interfaces. Through this, we hope to obtain robust evidence of MZMs in carefully designed tunnelling experiments that take into account what we learned in the past few years about the alternative origins for zero-bias peaks. On the way to qubit circuits and braiding, many interesting experiments await such as direct measurement of the fermion parity anomaly[10], or non-local correlations[40,41] and teleportation[42,43] associated with bulk topological superconductivity.

In the longer term, and perhaps more ambitiously, the same superconductor–semiconductor interfaces will inspire topological physics that goes beyond Majorana zero modes, and may offer pathways to universal topological quantum computing[60] or to quantum simulation of fundamental phenomena such as supersymmetry[61] and black holes[62]. Parafermions—generalizations of Majorana modes where the non-interacting nanowire is replaced with a fractional quantum Hall edge state—provide one example[63–65]. Parafermions can intuitively be thought of as fractionalized Majorana modes. They obey more complex non-Abelian rules that can perform the entire set of Clifford gates even without measurement. Parafermions have not been realized, but work on this topic must start from well-characterized superconductor-semiconductor two-dimensional interfaces. In order to enter the quantum Hall regime, superconductivity must withstand large out-of-plane magnetic fields, ruling out the use of aluminum with its critical field of order 10 mT. This provides another reason to experiment with other superconductor/semiconductor combinations in the near future. Van der Waals heterostructures featuring materials such as graphene and layered superconductors also hold great promise for the realization of parafermions, as superconductivity in the quantum Hall regime has already been demonstrated[66].

Topological superconductivity with the addition of Coulomb interactions has been a highly motivating topic for theorists and may lead to interesting experiments. Here we highlight an Ising topological phase[67–69] built from an array of interacting nanowires (Fig. 4a). This phase differs qualitatively from two-dimensional topological superconductors because it may contain visons, the vortices that bind Majorana modes. Visons are truly localized in contrast with Abrikosov or Josephson vortices that are associated with a non-local halo of phase winding. The Ising topological phase is interesting because it supports topological degeneracy, which arises from arranging these Majorana wires in a circuit with non-trivial topology even if there are no free ends. The Ising topological phase also leads to completely topologically protected quantum computing[60].

Another intriguing opportunity is to realize and study supersymmetry on a semiconductor chip[70]. Coulomb interactions in a one-dimensional chain lead to phase fluctuations, which invite the possibility of a topological version of a superconductor–insulator transition. It has recently been shown theoretically[61] that in specific limits, this transition can coincide with the topological superconducting phase transition leading to a combined supersymmetric critical point[71]. A symmetry that emerges at the critical point should connect the bosonic phase mode and the fermionic quasiparticle mode.

Another exotic phase that deserves attention is the so-called Sachdev–Ye–Kitaev model[72–74] based on four-Majorana interactions. This phase can be created when a large number of Majorana modes are forced to remain at zero energy by a special chiral symmetry (Fig. 4b). Coupling a bundle of wires to a disordered quantum dot can induce random Coulomb interactions between the MZMs that ultimately realizes the Sachdev–Ye–Kitaev model[62]. The

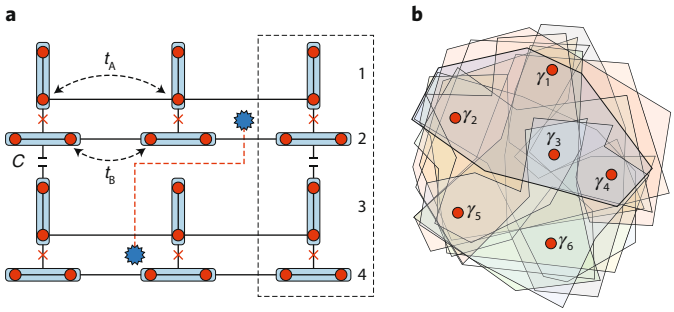


**Fig. 4 | Future exotic topologically superconducting phases. a**, Array of Coulomb-blockaded Majorana wires (MZMs shown as red dots) can be used to modulate the sign of the Majorana tunnelling leading to an emergent $\mathbb{Z}_2$ gauge field similar to an Ising topological phase. Sign-flip hopping around the red-dashed lines leads to a pair of local excitations (visons) shown by stars[60]. $t_A$, $t_B$, tunnel couplings; *C*, capacitance; red crosses, Josephson junctions. **b**, A cartoon representation of the Sachdev-Ye-Kitaev model which requires randomized four-way interactions (polygons) to dominate in a system of many MZMs (red circles, $\gamma$ symbols)[62]. Panel **a** adapted with permission from ref. [60].

model is remarkable from the theoretical point of view because it is one of the few strongly interacting solvable models that thermalizes. The model is particularly interesting as it scrambles quantum information at the maximal rate that is allowed[75]. This relates the behaviour of this system to conjectured quantum mechanical properties of black holes, potentially making them accessible in a table-top experiment.

Clearly, the effort to realize Majorana modes, quite apart from the potential for quantum computation, will likely have broader implications for understanding deeper concepts in quantum many-body physics. The path forward lies through improved understanding of materials science of superconductor/semiconductor interfaces, advanced quantum engineering and methodical partnership between experiment and theory.

Received: 12 September 2019; Accepted: 30 April 2020;
Published online: 7 July 2020

## References

1. Read, N. & Green, D. Paired states of fermions in two dimensions with breaking of parity and time-reversal symmetries and the fractional quantum hall effect. *Phys. Rev. B* **61**, 10267–10297 (2000).
2. Ivanov, D. A. Non-abelian statistics of half-quantum vortices in p-wave superconductors. *Phys. Rev. Lett.* **86**, 268–271 (2001).
3. Kitaev, A. Y. Fault-tolerant quantum computation by anyons. *Ann. Phys.* **303**, 2–30 (2003).
4. Volovik, G. E. Fermion zero modes on vortices in chiral superconductors. *J. Exp. Theor. Phys. Lett.* **70**, 609–614 (1999).
5. Fu, L. & Kane, C. L. Superconducting proximity effect and Majorana fermions at the surface of a topological insulator. *Phys. Rev. Lett.* **100**, 096407 (2008).
6. Lutchyn, R. M., Sau, J. D. & Das Sarma, S. Majorana fermions and a topological phase transition in semiconductor-superconductor heterostructures. *Phys. Rev. Lett.* **105**, 077001 (2010).
7. Oreg, Y., Refael, G. & von Oppen, F. Helical liquids and Majorana bound states in quantum wires. *Phys. Rev. Lett.* **105**, 177002 (2010).
8. Kitaev, A. Y. Unpaired Majorana fermions in quantum wires. *Phys. -Uspekhi* **44**, 131–136 (2001).
9. Sengupta, K., Žutić, I., Kwon, H.-J., Yakovenko, V. M. & Das Sarma, S. Midgap edge states and pairing symmetry of quasi-one-dimensional organic superconductors. *Phys. Rev. B* **63**, 144531 (2001).
10. Liu, C.-X., Cole, W. S. & Sau, J. D. Proposal for measuring the parity anomaly in a topological superconductor ring. *Phys. Rev. Lett.* **122**, 117001 (2019).
11. Krogstrup, P. et al. Epitaxy of semiconductor–superconductor nanowires. *Nat. Mater.* **14**, 400–406 (2015).
12. Shabani, J. et al. Two-dimensional epitaxial superconductor-semiconductor heterostructures: A platform for topological superconducting networks. *Phys. Rev. B* **93**, 155402 (2016).

13. Gazibegovic, S. et al. Epitaxy of advanced nanowire quantum devices. *Nature* **548**, 434–438 (2017).
14. Sugaya, T., Okada, Y. & Kawabe, M. Selective growth of GaAs by molecular beam epitaxy. *Jpn. J. Appl. Phys.* **31**, L713 (1992).
15. Nishinaga, T. & Bacchin, G. Selective area MBE of GaAs, AlAs and their alloys by periodic supply epitaxy. *Thin Solid Films* **367**, 6–12 (2000).
16. Mourik, V. et al. Signatures of Majorana fermions in hybrid superconductor-semiconductor nanowire devices. *Science* **336**, 1003–1007 (2012).
17. Das, A. et al. Zero-bias peaks and splitting in an Al-InAs nanowire topological superconductor as a signature of Majorana fermions. *Nat. Phys.* **8**, 887–895 (2012).
18. Deng, M. et al. Anomalous zero-bias conductance peak in a Nb–InSb nanowire–Nb hybrid device. *Nano. Lett.* **12**, 6414–6419 (2012).
19. Finck, A. D. K., Van Harlingen, D. J., Mohseni, P. K., Jung, K. & Li, X. Anomalous modulation of a zero-bias peak in a hybrid nanowire-superconductor device. *Phys. Rev. Lett.* **110**, 126406 (2013).
20. Churchill, H. O. H. et al. Superconductor-nanowire devices from tunneling to the multichannel regime: Zero-bias oscillations and magnetoconductance crossover. *Phys. Rev. B* **87**, 241401 (2013).
21. Lee, E. J. H. et al. Spin-resolved andreev levels and parity crossings in hybrid superconductor-semiconductor nanostructures. *Nat. Nanotechnol.* **9**, 79–84 (2014).
22. Liu, C.-X., Sau, J. D., Stanescu, T. D. & Das Sarma, S. Andreev bound states versus Majorana bound states in quantum dot-nanowire-superconductor hybrid structures: trivial versus topological zero-bias conductance peaks. *Phys. Rev. B* **96**, 075161 (2017).
23. Vuik, A., Nijholt, B., Akhmerov, A. R. & Wimmer, M. Reproducing topological properties with quasi-Majorana states. *SciPost Phys.* **7**, 061 (2019).
24. Kells, Meidan, G. D. & Brouwer, P. W. Near-zero-energy end states in topologically trivial spin-orbit coupled superconducting nanowires with a smooth confinement. *Phys. Rev. B* **86**, 100503 (2012).
25. Pan, H., Cole, W. S., Sau, J. D. & Das Sarma, S. Generic quantized zero-bias conductance peaks in superconductor-semiconductor hybrid structures. *Phys. Rev. B* **101**, 024506 (2020).
26. Brouwer, P. W. & Beenakker, C. W. J. Insensitivity to time-reversal symmetry breaking of universal conductance fluctuations with Andreev reflection. *Phys. Rev. B* **52**, 16772 (1995).
27. Altland, A. & Zirnbauer, M. R. Random matrix theory of a chaotic andreev quantum dot. *Phys. Rev. Lett.* **76**, 3420–3423 (1996).
28. Albrecht, S. M. et al. Exponential protection of zero modes in Majorana islands. *Nature* **531**, 206–209 (2016).
29. Deng, M. T. et al. Majorana bound state in a coupled quantum-dot hybrid-nanowire system. *Science* **354**, 1557–1562 (2016).
30. Chen, J. et al. Experimental phase diagram of zero-bias conductance peaks in superconductor/semiconductor nanowire devices. *Sci. Adv.* **3**, e1701476 (2017).
31. Nichele, F. et al. Scaling of Majorana zero-bias conductance peaks. *Phys. Rev. Lett.* **119**, 136803 (2017).
32. Kjaergaard, M. et al. Quantized conductance doubling and hard gap in a two-dimensional semiconductor–superconductor heterostructure. *Nat. Commun.* **7**, 12841 (2016).
33. Grivnin, A., Bor, E., Heiblum, M., Oreg, Y. & Shtrikman, H. Concomitant opening of a bulk-gap with an emerging possible majorana zero mode. *Nat. Commun.* **10**, 1940 (2019).
34. Chen, J. et al. Ubiquitous non-Majorana zero-bias conductance peaks in nanowire devices. *Phys. Rev. Lett.* **123**, 107703 (2019).
35. Rokhinson, L. P., Liu, X. & Furdyna, J. K. The fractional a.c. Josephson effect in a semiconductor–superconductor nanowire as a signature of Majorana particles. *Nat. Phys.* **8**, 795–799 (2012).
36. Houzet, M., Meyer, J. S., Badiane, D. M. & Glazman, L. I. Dynamics of majorana states in a topological Josephson junction. *Phys. Rev. Lett.* **111**, 046401 (2013).
37. Billangeon, P.-M., Pierre, F., Bouchiat, H. & Deblock, R. Ac Josephson effect and resonant Cooper pair tunneling emission of a single Cooper pair transistor. *Phys. Rev. Lett.* **98**, 216802 (2007).
38. Anselmetti, G. L. R. et al. End-to-end correlated subgap states in hybrid nanowires. Preprint at https://arxiv.org/abs/1908.05549 (2019).
39. Yu, P. et al. Non-majorana states yield nearly quantized conductance in superconductor-semiconductor nanowire devices. Preprint at https://arxiv.org/abs/2004.08583 (2020).
40. Akhmerov, A. R., Dahlhaus, J. P., Hassler, F., Wimmer, M. & Beenakker, C. W. J. Quantized conductance at the Majorana phase transition in a disordered superconducting wire. *Phys. Rev. Lett.* **106**, 057001 (2011).
41. Rosdahl, T. Ö., Vuik, A., Kjaergaard, M. & Akhmerov, A. R. Andreev rectifier: a nonlocal conductance signature of topological phase transitions. *Phys. Rev. B* **97**, 045421 (2018).
42. Fu., L. Electron teleportation via Majorana bound states in a mesoscopic superconductor. *Phys. Rev. Lett.* **104**, 056402 (2010).
43. Michaeli, K., Landau, L. A., Sela, E. & Fu, L. Electron teleportation and statistical transmutation in multiterminal Majorana islands. *Phys. Rev. B* **96**, 205403 (2017).
44. Motrunich, O., Damle, K. & Huse, D. A. Griffiths effects and quantum critical points in dirty superconductors without spin-rotation invariance: one-dimensional examples. *Phys. Rev. B* **63**, 224204 (2001).
45. Ren, H. et al. Topological superconductivity in a phase-controlled Josephson junction. *Nature* **569**, 93–98 (2019).
46. Fornieri, A. et al. Evidence of topological superconductivity in planar Josephson junctions. *Nature* **569**, 89–92 (2019).
47. Alicea, J., Oreg, Y., Refael, G., von Oppen, F. & Fisher, M. P. A. Non-abelian statistics and topological quantum information processing in 1D wire networks. *Nat. Phys.* **7**, 412–417 (2011).
48. Van Heck, B., Akhmerov, A. R., Hassler, F., Burrello, M. & Beenakker, C. W. J. Coulomb-assisted braiding of Majorana fermions in a Josephson junction array. *New. J. Phys.* **14**, 035019 (2012).
49. Karzig, T. et al. Scalable designs for quasiparticle-poisoning-protected topological quantum computation with Majorana zero modes. *Phys. Rev. B* **95**, 235305 (2017).
50. Stenger, J. P. T., Hatridge, M., Frolov, S. M. & Pekker, D. Braiding quantum circuit based on the 4π Josephson effect. *Phys. Rev. D.* **99**, 035307 (2019).
51. Krizek, F. et al. Field effect enhancement in buffered quantum nanowire networks. *Phys. Rev. Mater.* **2**, 093401 (2018).
52. Aseev, P. et al. Selectivity map for molecular beam epitaxy of advanced III–V quantum nanowire networks. *Nano Lett.* **19**, 218–227 (2018).
53. Lee, J. S. et al. Selective-area chemical beam epitaxy of in-plane InAs one-dimensional channels grown on InP (001), InP (111) B, and InP (011) surfaces. *Phys. Rev. Mater.* **3**, 084606 (2019).
54. Friedl, M. et al. Template-assisted scalable nanowire networks. *Nano Lett.* **18**, 2666–2671 (2018).
55. Rainis, D. & Loss, D. Majorana qubit decoherence by quasiparticle poisoning. *Phys. Rev. B* **85**, 174533 (2012).
56. Lafarge, P., Joyez, P., Esteve, D., Urbina, C. & Devoret, M. H. Measurement of the even-odd free-energy difference of an isolated superconductor. *Phys. Rev. Lett.* **70**, 994–997 (1993).
57. Pendharkar, M. et al. Parity-preserving and magnetic field resilient superconductivity in indium antimonide nanowires with tin shells. Preprint at https://arxiv.org/abs/1912.06071 (2019).
58. Bjergfelt, M. et al. Superconducting vanadium/indium-arsenide hybrid nanowires. *Nanotechnology* **30**, 294005 (2019).
59. Carrad, D. J. et al. Shadow lithography for in-situ growth of generic semiconductor/superconductor devices. Preprint at https://arxiv.org/abs/1911.00460 (2019).
60. Barkeshli, M. & Sau, J. D. Physical architecture for a universal topological quantum computer based on a network of Majorana nanowires. Preprint at https://arxiv.org/abs/1509.07135 (2015).
61. Ebisu, H., Sagi, E. & Oreg, Y. Supersymmetry in the insulating phase of a chain of majorana cooper pair boxes. *Phys. Rev. Lett.* **123**, 026401 (2019).
62. Chew, A., Essin, A. & Alicea, J. Approximating the Sachdev-Ye-Kitaev model with Majorana wires. *Phys. Rev. B* **96**, 121119 (2017).
63. Clarke, D. J., Alicea, J. & Shtengel, K. Exotic non-abelian anyons from conventional fractional quantum Hall states. *Nat. Commun.* **4**, 1348 (2013).
64. Lindner, N. H., Berg, E., Refael, G. & Stern, A. Fractionalizing majorana fermions: Non-abelian statistics on the edges of abelian quantum hall states. *Phys. Rev. X* **2**, 041002 (2012).
65. Cheng, M. Superconducting proximity effect on the edge of fractional topological insulators. *Phys. Rev. B* **86**, 195126 (2012).
66. Amet, F. et al. Supercurrent in the quantum Hall regime. *Science* **352**, 966–969 (2016).
67. Moore, G. & Read, N. Nonabelions in the fractional quantum Hall effect. *Nucl. Phys. B* **360**, 362–396 (1991).
68. Kitaev, A. Anyons in an exactly solved model and beyond. *Ann. Phys.* **321**, 2–111 (2006).
69. Yao, H. & Kivelson, S. A. Exact chiral spin liquid with non-abelian anyons. *Phys. Rev. Lett.* **99**, 247203 (2007).
70. Wess, J. & Bagger, J. *Supersymmetry and supergravity* (Princeton Univ. Press, 1992).
71. Friedan, D., Qiu, Z. & Shenker, S. H. Conformal invariance, unitarity and two-dimensional critical exponents. *Phys. Rev. Lett.* **52**, 1575–1578 (1984).
72. Sachdev, S. & Ye, J. Gapless spin-fluid ground state in a random quantum Heisenberg magnet. *Phys. Rev. Lett.* **70**, 3339–3342 (1993).
73. Kitaev, A. *A Simple Model Of Quantum Holography (Part 1)* http://online.kitp.ucsb.edu/online/entangled15/kitaev/ (UC Santa Barbara, 2015).
74. Kitaev, A. *A Simple Model Of Quantum Holography (Part 2)* http://online.kitp.ucsb.edu/online/entangled15/kitaev2/ (UC Santa Barbara, 2015).
75. Maldacena, J., Shenker, S. H. & Stanford, D. A bound on chaos. *J. High. Energy Phys.* **2016**, 106 (2016).

## Acknowledgements
We thank S. Das Sarma for comments. S.M.F. is supported by NSF DMR-1906325, NSF PIRE-1743717, ONR and ARO. M.J.M is supported by Microsoft Quantum. J.S. is supported by the NSF-DMR1555135 and helpful discussions at the KITP under Grant no. NSF PHY-1748958.

## Competing interests
The authors declare no competing interests.

## Additional information
**Correspondence** should be addressed to S.M.F.

**Reprints and permissions information** is available at www.nature.com/reprints.

**Publisher's note** Springer Nature remains neutral with regard to jurisdictional claims in published maps and institutional affiliations.